

Design of a Test Facility for Vibration Isolator Characterisation

J. D. Dickens, and C. J. Norwood

Ship Structures and Materials Division
Aeronautical and Maritime Research Laboratory, DSTO
506 Lorimer Street, Fishermens Bend, 3207

ABSTRACT: Vibration isolators are an important element in the reduction of structure-borne noise transmission. The dynamic properties need to be determined at the pre-load and over the frequency range experienced in normal operation. The four-pole parameters description of the isolator dynamic properties is independent of the testing arrangement. A test facility has been designed to measure the four-pole parameters of vibration isolators with pre-loads up to 30 kN and over a frequency range from 10 Hz to 2000 Hz. This paper describes the dynamic design of the test facility using modal analysis and harmonic response analysis.

1. INTRODUCTION

The vibratory power transmitted from machinery mounted on isolators depends upon the dynamic properties of the foundation, the machinery mounting point and the vibration isolation mounts. A knowledge of the frequency dependent dynamic properties of vibration isolators is necessary in order to be able to predict their isolation performance. In particular for naval surface ships and submarines determination of the vibration characteristics is vital for acoustic signature management.

Most isolators contain elastomeric material, the stiffness and damping properties of which are both frequency and pre-load dependent. In addition it is possible for standing waves to be set up within the isolator at certain frequencies, which greatly reduce its effectiveness at those frequencies. It is therefore necessary to determine the isolator properties under the pre-load conditions and frequency range experienced in normal operation.

The transfer impedance or mobility of an isolator has traditionally been used to describe its dynamic properties and provide a measure of its isolation performance. This measure does not necessarily provide a full description and may also be dependent upon the test conditions. An alternative description is provided by the four-pole parameters, which relate the force and velocity above the isolator to the force and velocity below. This parameter set is particularly adapted to analysing composite systems.

The significance of the four-pole parameter description is that it provides a measure of the isolator dynamic properties that is not dependent upon the measuring set-up, and it can be used to give an estimate of the isolator's effectiveness.

A vibration isolator test facility was developed at the Aeronautical and Maritime Research Laboratory to measure the frequency dependent vibration transmission characteristics of flexible isolation mounts used for machinery

on-board ships and submarines. The test facility has been designed to measure the four-pole parameters at pre-loads of up to 30 kN and over the frequency range from 10 Hz to 2000 Hz. In undertaking the experimental measurements the force and velocity above and below the isolator need to be determined, and it is vital that the dynamics of the testing machine structure do not affect the results.

This paper describes the modelling of the modal behaviour of the elements of the test rig and the use of harmonic response analysis modelling to ensure there is no effect on the experimental measurements from the structural modes of the test rig. The results show that while the structural framework and other elements of the test rig have natural modes within the frequency range of interest, careful design can ensure that these do not affect the results.

2. FOUR-POLE PARAMETERS

The four-pole parameters description of the dynamic properties of a vibration isolator relates the forces F_1 and velocity V_1 at the isolator's input to the force F_2 and velocity V_2 at the isolator's output, $[1, 2, 3]$ is

$$\begin{bmatrix} F_1 \\ V_1 \end{bmatrix} = \begin{bmatrix} \alpha_{11} & \alpha_{12} \\ \alpha_{21} & \alpha_{22} \end{bmatrix} \begin{bmatrix} F_2 \\ V_2 \end{bmatrix} \quad (1)$$

where α_{11} , α_{12} , α_{21} , and α_{22} are the four-pole parameters, and are complex, time-invariant functions of the angular frequency ω .

Application of Maxwell's law of reciprocal deflections to the isolator leads to the relationship:

$$\alpha_{11}\alpha_{22} - \alpha_{12}\alpha_{21} = 1 \quad (2)$$

A symmetric isolator is one that behaves the same if the input and output ports are interchanged. For this case an additional relation is applicable:

$$\alpha_{11} = \alpha_{22} \quad (3)$$

From equations (2) and (3) it is evident that, for a symmetric isolator, only two independent four-pole parameters need to be measured in order to completely characterise it. At lower frequencies an isolator may be assumed to be a massless spring of dynamic stiffness k . This assumption yields $\alpha_{11} = \alpha_{22} = 1$, $\alpha_{12} = 0$ and $\alpha_{21} = j\omega/k$, where $j = \sqrt{-1}$ and ω is the circular frequency.

From equation (1) two particular cases can be derived. Case 1 is for the output to be free, $F_2 = 0$, which yields $F_1 = \alpha_{12}V_2$ and $V_1 = \alpha_{22}V_2$. Case 2 is for the output blocked, $V_2 = 0$, which yields $F_1 = \alpha_{11}F_2$ and $V_1 = \alpha_{21}F_2$. While the first case is experimentally convenient it does not allow the determination of the isolator properties under pre-load, and therefore the properties measured in this way will not be representative of those for the installed isolator.

Verheij [4] developed a method for determining the blocked transfer function $F_2/j\omega V_1$. Dickens and Norwood [5] developed a system that followed Verheij's basic method but determined the four-pole parameters. Improvements to the original measurement technique correcting for the small but finite velocity of the blocking mass, and measuring the force directly were suggested by Dickens and Norwood, [6, 7]. It was decided to implement these measurement improvements in an upgraded test rig. Additional improvements would also include increasing the upper frequency limit to 2 kHz and the dynamic force capacity to 5.3 kN.

3. TEST RIG

The developed test rig is shown schematically in Figure 1. The test isolator under test is mounted between two large masses; static pre-load is applied by air-bags top and bottom and the dynamic load by an electro-dynamic shaker. The rig has two supporting frames, the upper frame that supports the shaker and the lower frame that provides the reaction forces for the upper pre-loading air-bags. The lower pre-loading air-bags sit on a base plate mounted on top of a seismic mass.

Two frames are used to reduce coupling between the pre-loading structure and the shaker. The shaker is decoupled from its supporting frame by four isolation hangers and drives the excitation mass through a single centrally located connecting rod. The seismic mass is a block of reinforced concrete of dimensions $3\text{m} \times 3\text{m} \times 1\text{m}$, supported on four air-bags connected to air reservoirs and having a mounted natural frequency of approximately 1.2 Hz. The use of the seismic mass decouples the blocking mass from the laboratory floor, reducing the input of extraneous forces and transmissions from the two supporting frames.

Air-bags are used to provide the pre-load as the static force can be easily adjusted, while at the same time giving a degree of isolation between the masses and the supporting structure. The dynamic force between the excitation mass and the isolator is measured directly by an assembly of force transducers. The motions of the excitation and blocking masses are measured using accelerometers.

The rig was required to be able to test isolators with

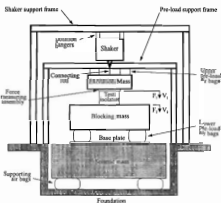


Figure 1. Schematic of Vibration Isolation Test Rig.

dynamic stiffnesses in the range from 1×10^5 to 2×10^7 N/m, with pre-loads adjustable over the range from 1.5 to 30 kN and over a frequency range from 10 to 2000 Hz. In designing the test rig it was important that the dynamic response of the test rig did not affect the measurement of the isolator's four-pole parameters. This implies that where possible the components of the test rig should not have structural modes within or near the frequency band of interest, and where this is not possible the structural response of the rig should not affect the results.

4. DYNAMIC ANALYSIS OF THE TEST RIG

The analysis is divided into three parts. Firstly modal analyses were conducted to determine the natural frequencies and mode shapes of the test rig components and sub-components. Where possible, components were designed not to have structural modes within or near the test frequency band; these included the excitation mass, the blocking mass, the table extension for the shaker, the force measuring assembly and the base plate for the seismic mass.

For components that could not be designed to satisfy the modal frequency criterion, a harmonic response analysis was performed. The effect of the modal behaviour of the various components on the measurements was determined. Items in this group included the supporting frames and the seismic mass.

Finally a harmonic response analysis for the entire assembly was performed and compared with the response from an idealised spring/mass system. This was done to ascertain if there were any effects from the modal behaviour of the individual test rig components on the assembly as a whole.

The ANSYS finite element analysis program was used in the analyses.

4.1 Modal Analyses

In this series of analyses the natural frequencies and mode shapes of the excitation mass, blocking mass, shaker table extension and the air bag base plate were determined to ensure they did not occur within the frequency range of interest. The components were modelled using eight noded brick elements, and where necessary, the parts of the test rig in contact with

the component under study were included in the model to ensure appropriate boundary conditions.

(a) *Blocking mass*: The model included the supporting air-bags and the isolator. Two extreme cases were considered, the stiffest isolator under the maximum pre-load and the softest isolator under the minimum pre-load. The air-bags and the isolator were modelled as springs spread over the contact areas. The optimum design selected for the blocking mass was a steel cylinder of diameter 480 mm and height 398 mm, which gave a first modal frequency of 4.00 kHz for the (1,0) mode. To apply the two mass method described by Dickens and Norwood [2] for testing non-symmetric isolators, two different blocking masses are required. A second blocking mass made from an aluminium alloy was analysed to ensure its modal properties were adequate. It had the same height but a smaller diameter compared to the first mass, and slightly higher predicted modal frequencies.

(b) *Excitation mass*: This model included the pre-loading air-bags and the isolator. As for the blocking mass the air-bags and isolator were modelled as spring elements, and the two extreme cases described above were analysed. Similarly to the blocking mass, the optimum shape selected was a cylinder; in this case it had a diameter of 360 mm and a height of 355 mm, with the first natural frequency of 4.58 kHz. The first mode was torsional, and the second mode was the (1,0) mode at 5.66 kHz. To accommodate low pre-loading forces down to 1.5 kN, a second excitation mass having a lower mass was required. The second mass had the same dimensions as the first excitation mass but was made from an aluminium alloy, and gave marginally higher predicted modal frequencies.

(c) *Base extension*: In order to limit the length of the rod connecting the shaker's table to the excitation mass, it was necessary to provide an extension to the shaker table. This would be bolted to the shaker table in six locations and was required to have a minimum height of 175 mm. The extension was made of aluminium to minimise its mass. The optimum design selected was a base cylinder of diameter 125 mm leading into a cone and tapering to a 20 mm diameter cylinder at the top. This had a first mode at 4.26 kHz.

(d) *Base plate*: A base plate attached to the seismic mass was to be used to locate the six lower pre-loading air-bags under the blocking mass. The diameter of the plate was set at 480 mm diameter, which was the minimum required to support the air-bags. The plate was initially modelled as being attached to the seismic mass by 15 bolts on three concentric circles. The optimum solution for this arrangement was a steel plate with thickness of 45 mm giving a first mode at 3.57 kHz. One of the problems to be resolved with this model was that the mode shape would be rectified. The plate could deflect away from the mass only. Unfortunately this one-way motion was not able to be modelled, so the mode shapes were calculated as for normal bi-directional deflection. It was reasoned that the uni-directional motion constraint would increase the modal frequency so the results calculated would be conservative.

A second model using adhesive to attach the plate to the

seismic mass was made. This consisted of a plate 40 mm thick and three locating bolts, with a continuous layer of epoxy adhesive between the plate and the mass. The adhesive layer was modelled as a continuous compliant layer and the first structural frequency was 11.86 kHz. This design was selected in the construction of the test rig.

4.2 Harmonic Response Analyses

The harmonic responses of the two support frames and the seismic mass were modelled to ensure that the modes which occur within the desired test frequency range did not affect the results. The two frames were modelled using three dimensional beam elements, and the seismic mass was modelled using eight noded brick elements. Initially the modal analysis was performed and then the harmonic response analysis was performed using modal superposition, with clustering at the modal frequencies to give better resolution of the expected peak responses. The forcing function modelled the input from the shaker, and each analysis was carried out using several different damping conditions to assess the importance of damping to the peak responses.

(a) *Shaker support frame*: The model of the frame included the columns, cross beams and braces for the frame itself and the isolation hangers on which the shaker was supported. The shaker was modelled as a lumped mass and the input force was applied to it. The response analysis was designed to determine the level of force transmitted to the floor by the frame, and hence the amount of feedback to the air-bags supporting the blocking mass through the seismic mass. The reaction forces at the base of the columns were calculated, and multiplied by the measured transfer function between the mounting points for the columns on the floor and the top of the seismic block.

The displacements predicted by this method were at least 120 dB less than those predicted on the seismic block via the direct path through the isolator and the blocking mass over the frequency range of interest. Therefore it was concluded that feedback via the shaker supporting frame was not a problem.

(b) *Pre-load support frame*: The pre-load support frame consisted of a pair of portal frames cross connected by an "H" structure which carried the pre-loading air-bags. The model included the upper and lower pre-loading air-bags, the excitation mass, isolator, blocking mass, seismic mass and supporting air-bags. The air-bags and isolator were modelled as spring elements and the masses were modelled as rigid mass elements. The system was excited by applying an harmonic force to the excitation mass. The analysis was intended to predict the errors caused by the feedback of the reaction forces at the base of the supporting frame columns via the laboratory floor and the seismic mass' base.

The calculated reaction forces were combined with measured transfer functions to predict the displacements on the top of the seismic mass. Over the frequency range of interest it was found that the predicted displacement peaks due to the feedback path were at least 90 dB below the amplitude of those due to the forward path via the blocking

mass. This shows that the pre-load support frame is more important than the shaker support frame as a potential error path. However the levels predicted are so far below the displacement levels via the forward path that errors due to feedback through the frame will not be significant.

(c) *Seismic mass*: A modal analysis of the seismic mass showed that it had a considerable number of modes below 2 kHz, so that the important consideration would be that these modes did not affect the results. It is also possible for the seismic mass to be excited by the forward path forces through the pre-loading air-bags under the blocking mass, and these motions could affect the results. Therefore a model of the seismic mass, excitation mass, base plate, blocking mass, adhesive layer, locating bolts, air-bags and isolator was made. The seismic mass, base plate and blocking mass were modelled using eight-noded brick elements and the excitation mass was modelled as a lumped mass, while the air-bags and the isolator were idealised as spring elements.

This was compared to an idealised system where the seismic mass modelled as a rigid mass element and its supporting air-bags combined together. In addition, the bottom of the adhesive layer in contact with the seismic mass was constrained to move rigidly in sympathy with the seismic mass. The other elements in the model remained the same as above.

The displacements on the blocking mass and the contact forces between the blocking mass and the isolator for the actual system were compared for the two models. For the two models the displacements and forces differed by less than 0.03% and 0.01% respectively, indicating that the modal behaviour of the seismic mass has an insignificant effect on both the predicted displacements and forces.

5. MODELLING AND ANALYSIS FOR COMPLETE SYSTEM

The system was idealised as a series of springs and rigid masses to determine the system frequencies and establish if these modes would affect the measurements, Figure 2. The model didn't include the supporting frames, so the stiffness elements attached to the frames were assumed to be fixed at these points.

The isolation hangers are made up of multi-layer rubber isolation elements and steel springs and are represented by the springs k_1 and k_2 and the mass m_1 . The shaker is made up of the trunnion, body, driving magnetic coil and extension table and is represented by the masses m_2 , m_3 , m_4 and m_5 and by the springs k_3 , k_4 and k_5 . The force F_{in} produced by the shaker is generated between the body and the driving magnetic coil.

The shaker drives the excitation mass through a connecting rod, represented by the spring k_6 , while the upper pre-loading air-bags are modelled by k_7 . The excitation mass including the top mass of the force measuring assembly, the mass of the end supports for the pre-loading air-bags and one half of the air bag mass is represented by m_6 . The stiffness of the force measuring assembly is modelled by the spring k_8 .



Figure 2. Spring-mass representation of Test Rig.

The isolator under test is considered to comprise upper and lower plates separated by an elastomeric element represented by the stiffness k_9 . The mass m_7 includes the upper plate, the bottom plate of the force measuring assembly plus half the mass of the elastomer. The blocking mass, isolator lower plate, half of the elastomer mass, the masses of the end supports for the air-bags and half of the masses of the supporting air-bags are represented by mass m_8 . The stiffness of the air-bags is modelled by k_{10} . The mass m_9 represents the seismic mass, base plate, mass of the end supports for the air-bags and half the mass of the supporting air-bags. The spring k_{11} represents the stiffness of the air-bags that support the seismic mass.

Two limiting cases need to be considered. The softest case, comprising the softest expected isolator under minimum pre-load with the lighter excitation mass; and the stiffest case, comprising the stiffest expected isolator under maximum pre-load and with the heavier excitation mass. It is not possible to know a priori the masses of all the isolators to be tested, representative minimum and maximum masses were selected from isolators already tested.

The system as modelled has nine degrees of freedom and hence nine modal frequencies. The modal frequencies were solved for using MATLAB software. Masses and stiffnesses for the two limiting cases investigated are given in Tables 1 and 2 and the modal frequencies are given in Table 3.

Modes 4, 5, 6, 7 and 8 fall near or within the desired frequency range of measurement from 10 Hz to 2 kHz. The fourth mode has the table, coil, excitation mass and the top plate of the isolator in-phase with each other, but out-of-phase with the isolator's bottom plate and blocking mass. The

stiffness of the isolator has a major influence on the modal frequency f_4 . The hanger exhibits the dominant motion in the fifth mode, and is out-of-phase with the trunnion. The frequency f_5 is determined by the stiffnesses of the rubber and steel spring elements, and thus is the same for both cases. In the sixth mode, the table and coil are in-phase with each other and out-of-phase with the excitation mass. The frequency f_6 is predominantly determined by the stiffness k_6 of the connecting rod. In the seventh mode, the shaker's trunnion is out-of-phase with its body and the frequency f_7 critically depends on the stiffness of the toroidal elastomeric isolators, and remains the same for both cases. The table and coil are out-of-phase with each other in the eighth mode, and the frequency f_8 is critically dependant upon the stiffness k_5 , and so is equal for both cases.

Table 1
Masses

Mass (kg)	m_1	m_2	m_3	m_4	m_5	m_6	m_7	m_8	m_9
Softest case	16.6	41.1	607	4.34	6.38	109	1.65	572	22200
Stiffest case	16.6	41.1	607	4.34	6.38	292	10.3	581	22200

Table 2
Stiffnesses

Stiffness (N/m)	k_1	k_2	k_3	k_4	k_5	k_6	k_7	k_8	k_9	k_{10}	k_{11}
Softest case	1.57 $\times 10^3$	1.63 $\times 10^3$	2.65 $\times 10^3$	1.37 $\times 10^2$	5.49 $\times 10^2$	6.77 $\times 10^2$	2.62 $\times 10^4$	2.00 $\times 10^2$	1.00 $\times 10^2$	2.31 $\times 10^2$	2.87 $\times 10^2$
Stiffest case	1.57 $\times 10^3$	1.63 $\times 10^3$	2.65 $\times 10^3$	1.37 $\times 10^2$	5.49 $\times 10^2$	6.77 $\times 10^2$	4.37 $\times 10^3$	3.00 $\times 10^2$	2.00 $\times 10^2$	7.80 $\times 10^2$	2.87 $\times 10^2$

Table 3
Natural frequencies

Frequency (Hz)	f_1	f_2	f_3	f_4	f_5	f_6	f_7	f_8	f_9
Softest case	1.80	2.72	3.74	7.75	156	410	1320	2370	5580
Stiffest case	1.88	3.31	6.30	50.2	156	399	1320	2370	2770

From the work by Dickens and Norwood [3] and since the direct force at the input of the sample isolator is being measured, modes 4, 5, 6, 7 and 8 will not adversely affect the test measurements. The sixth and eighth modes dominate the behaviour of the excitation mass, which shows maximum acceleration levels at the frequencies f_6 and f_8 . When testing at or near these frequencies, care must be exercised to prevent excessive acceleration and force amplitudes of the table and coil. The upper frequency limit of the measurements is determined by the modal behaviour of the assembly of force

transducers used to measure the input force, given by the ninth mode. In this mode the excitation mass and the top mass of the assembly are in-phase with each other but out of phase with the bottom mass of the assembly and the top plate of the isolator. The force transducer assembly measures the direct forces satisfactorily until it exhibits modal behaviour, and so the upper limit is determined by f_9 , which predominantly depends upon the axial stiffnesses of the force transducers and the masses of the isolator's top end plate and elastomer. Therefore the upper frequency limits of the measurements for the softest and stiffest cases are 5.58 and 2.77 kHz, respectively.

Dickens and Norwood [3] derived an expression for the lower frequency limit of the measurements using direct forces. This limit is governed by the square root of the sum of the stiffnesses of the isolator and the lower pre-loading air-bags divided by the sum of the masses of the blocking mass and the isolator's lower plate. For the softest and stiffest cases they equate to 3.83 and 30.1 Hz, respectively.

Allowing factors of approximately two for the lower, and one half for the upper frequency limits gives practical testing frequency ranges for the softest and stiffest cases of 10 Hz to 2.7 kHz, and 60 Hz to 1.3 kHz, respectively. Because the modal behaviour of the individual components of the system has been designed for a maximum frequency of 2.00 kHz, the resulting system frequency ranges for the softest and stiffest cases are 10 Hz to 2.0 kHz, and 60 Hz to 1.3 kHz, respectively.

6. CONCLUDING REMARKS

A test facility has been designed to measure the four-pole parameters of vibration isolators with pre-loads of up to 30 kN. The frequency range over which the isolators can be tested is not limited by the structure and construction of the test rig. The lower frequency is governed by the stiffness of the isolator and the lower pre-load air-bags, and the masses of the blocking mass and the isolator's lower plate, and not the structure of the test rig. The only components of the test facility with modal behaviour in the frequency range of interest are the two frames and the seismic mass. The flanking path transmission from the isolator input to the output through the frames, the ground and the seismic mass is at least 90 dB lower than the direct path excitation level. Therefore the modal behaviour of the frames will not influence the test results. The effect of the modal behaviour of the seismic mass on the measured isolator's velocities and forces is predicted to be less than 0.03% and 0.01% respectively, and so can be considered negligible.

The test rig will be used to measure the four-pole parameters of isolators used to control the structure-borne noise transmission in ships and submarines. Using the four-pole parameters and the dynamic properties of the structure above and below the isolator, the effectiveness of the isolator can be determined. An isolator's performance will change

over time and with exposure to environmental factors such as oil and heat. The test rig will be used to measure the four-pole parameters for new and aged isolators to determine the degradation and the allowable life between refit. The performance of purpose designed isolators can be determined with the test rig providing a more comprehensive measure of the isolators performance than quality control tests now used.

REFERENCES

1. C.T. Molloy, "Use of four-pole parameters in vibration calculations," *J. Acoust. Soc. Am.* **29**, 842-853 (1957).
2. J.C. Snowdon, "Vibration isolation: Use and characterisation," *J. Acoust. Soc. Am.* **66**, 1245-1274 (1979).
3. J.D. Dickens, C.J. Norwood and R.G. Juniper, "Four pole parameter characterisation of isolator acoustic

transmission performance," *Proc. Aust. Acoust. Soc. Conf.*, Glenelg, SA, 1993. pp. 110-117.

4. J.W. Verheij, *Multi-path sound transfer from resiliently mounted shipboard machinery*, Ph.D. thesis, Institute of Applied Physics TNO-TH, Delft, (1982).
5. J.D. Dickens and C.J. Norwood, Vibration isolator test facility, *Defence Science and Technology Organisation, Aeronautical and Maritime Research Laboratory*, report DSTO-TR-0357, (1996).
6. J.D. Dickens and C.J. Norwood, Measurement of four-pole parameters using blocking masses, *Proc. Aust. Acoust. Soc. Conf.*, Canberra, ACT, 1994. pp. 57-65.
7. J.D. Dickens and C.J. Norwood, Measurement of four-pole parameters using direct forces, *Proc. Aust. Acoust. Soc. Conf.*, Fremantle, WA, 1995. pp. 15-21.



A Hand-Held Analyser at under \$8,000 Impossible!

SVAN 912 - Multi-function Hand-Held Analyser



- Sound Level Meter
- Real Time Analyser
- Vibration Analyser

*A dedicated instrument
unique in the market
place. An ideal
diagnostic tool*

- Portable
- Multi-function
- FFT Real Time
- Zoom Function
- Type 1
- 1/1-1/3 Octave
- Narrow Band
- Human Vibrations
- Low Cost
- Battery Operated

*Calibrations
Sales, Hire
Repairs, Advice
Compare our low prices*

ACU-VIB Electronics
Acoustic and Vibration Electronics



Reg. Lab. No. 9262
Acoustic and Vibration
Measurements

56A Thompson Street
Drummoyne, NSW 2047
Tel: 018 470 179
Tel/Fax: (02) 9819 6398
PO Box W16
Waremba, NSW 2046